2005

Mechanistic differences in RNA-dependent DNA polymerization and fidelity between murine leukemia virus and HIV-1 reverse transcriptases

Mark Skasko

Kellie K. Weiss

Holly M. Reynolds

Varuni Jamburuthugoda
SUNY Geneseo

Kwi Lee

See next page for additional authors

Recommended Citation

Skasko M., Weiss K.K., Reynolds H.M., Jamburuthugoda V., Lee K., Kim B. (2005) Mechanistic differences in RNA-dependent DNA polymerization and fidelity between murine leukemia virus and HIV-1 reverse transcriptases. Journal of Biological Chemistry 280: 12190-12200. doi: 10.1074/jbc.M412859200

THE JOURNAL OF BIOLOGICAL CHEMISTRY
Vol. 280, No. 13, Issue of April 1, pp. 12190–12200, 2005
Printed in U.S.A.

Mechanistic Differences in RNA-dependent DNA Polymerization and Fidelity between Murine Leukemia Virus and HIV-1 Reverse Transcriptases*

Received for publication, November 15, 2004, and in revised form, December 28, 2004
Published, JBC Papers in Press, January 10, 2005, DOI 10.1074/jbc.M412859200

Mark Skasko‡§, Kellie K. Weiss‡§, Holly M. Reynolds‡, Varuni Jamburuthugoda¶, Kwi Lee‡, and Baek Kim‡‖

From the Departments of ‡Microbiology and Immunology and ¶Biochemistry and Biophysics, University of Rochester, Rochester, New York 14642

We compared the mechanistic and kinetic properties of murine leukemia virus (MuLV) and human immunodeficiency virus type 1 (HIV-1) reverse transcriptases (RTs) during RNA-dependent DNA polymerization and mutation synthesis using pre-steady-state kinetic analysis. First, MuLV RT showed 6.5–121.6-fold lower binding affinity (K_d) to deoxynucleotide triphosphate (dNTP) substrates than HIV-1 RT, although the two RTs have similar incorporation rates (k_{pol}). Second, compared with HIV-1 RT, MuLV RT showed dramatic reduction during multiple dNTP incorporations at low dNTP concentrations. Presumably, due to its low dNTP binding affinity, the dNTP binding step becomes rate-limiting in the multiple rounds of the dNTP incorporation by MuLV RT, especially at low dNTP concentrations. Third, similar fold differences between MuLV and HIV-1 RTs in the K_d and k_{pol} values to correct and incorrect dNTPs were observed. This indicates that these two RT proteins have similar misinsertion fidelities. Fourth, these two RT proteins have different mechanistic capabilities regarding mismatch extension. MuLV RT has a 3.1-fold lower mismatch extension fidelity, compared with HIV-1 RT. Finally, MuLV RT has a 3.8-fold lower binding affinity to mismatched template/primer (T/P) substrate compared with HIV-1 RT. Our data suggest that the active site of MuLV RT has an intrinsically low dNTP binding affinity, compared with HIV-1 RT. In addition, instead of the misinsertion step, the mismatch extension step, which varies between MuLV and HIV-1 RTs, contributes to their fidelity differences. The implications of these kinetic differences between MuLV and HIV-1 RTs on viral cell type specificity and mutagenesis are discussed.

Retroviruses encode a versatile DNA polymerase called reverse transcriptase (RT).[1] The function of RT is to synthesize linear double-stranded proviral DNAs from single-stranded positive sense viral RNA genomes during viral replication. In order to catalyze this process, RTs perform several distinct enzymatic reactions including RNA-dependent DNA polymerization, DNA-dependent DNA polymerization, strand transfer, and RNase H cleavage (1). The DNA polymerase activity of RTs has been targeted, using various types of RT inhibitors such as nucleoside substrate-like compounds (*i.e.* azidothymidine (AZT) and didanosine (ddI)) (2), as a means to reduce viral replication in infected individuals. Lentiviruses such as human immunodeficiency virus type 1 (HIV-1) uniquely infect terminally differentiated/nondividing cells (*i.e.* macrophages) as well as dividing cells (*i.e.* activated CD4+ T cells), whereas oncoretroviruses such as murine leukemia virus (MuLV) productively replicate mainly in dividing cells (3, 4). Numerous studies have reported that actively dividing cells have higher cellular deoxynucleotide triphosphate (dNTP) concentrations than nondividing cells (5). Recently, it was reported that the cellular dNTP concentration of human macrophages (~40 nM) is ~100 times lower than that of dividing CD4 + T cells (~5 μM) (6). Therefore, RTs from these two major groups of animal retroviruses may execute proviral DNA synthesis at very different cellular dNTP availability.

RT of MuLV is the most extensively studied oncoretroviral RT. Kinetic and structural features of MuLV RT have been compared with those of HIV-1 RT, which is the most characterized lentiviral RT. These two RTs share many similarities in their enzymatic and molecular characteristics. Mutational analyses of conserved amino acid residues between these two RTs also demonstrate their functional resemblances. Interestingly, however, several key enzymatic differences exist between these two RTs. Firstly, we and others have reported that MuLV RT has higher steady-state K_m values to natural dNTPs than HIV-1 RT, although this difference varies, depending on the types of substrates and assays used (6–11). This suggests that HIV-1 RT efficiently incorporates dNTPs even at low dNTP concentrations, compared with MuLV RT. We recently postulated that the K_m difference between these two RTs may be related to the large cellular dNTP concentration difference observed between cell types that lentiviruses and oncoretroviruses specifically infect (6). It is possible that the low K_m value of HIV-1 RT enables HIV-1 to efficiently synthesize proviral DNA even in macrophages containing very low cellular dNTP concentrations. Like HIV-1 RT, simian immunodeficiency virus (SIV) RT also displays low fidelity and relatively low K_m values (12). However, mechanisms involved in these K_m differences remain to be explored.

Secondly, the M13 *lacZα* mutation assay demonstrated that MuLV RT has a 15-fold higher fidelity than HIV-1 RT (13). Various steady-state kinetic analyses also demonstrated that

* This work was supported by Grant AI49781 (to B. K.) and Training Grant AI07362 (to K. K. W.) from the National Institutes of Health. The costs of publication of this article were defrayed in part by the payment of page charges. This article must therefore be hereby marked "*advertisement*" in accordance with 18 U.S.C. Section 1734 solely to indicate this fact.

§ Both authors contributed equally to this work.
‖ To whom correspondence should be addressed: Dept. of Microbiology and Immunology, University of Rochester Medical Center, 601 Elmwood Ave., Box 672, Rochester, NY 14642. Tel.: 585-275-6916; Fax: 585-473-9573; E-mail: baek_kim@urmc.rochester.edu.

[1] The abbreviations used are: RT, reverse transcriptase; MuLV, murine leukemia virus; HIV-1, human immunodeficiency virus type 1; dNTP, deoxynucleotide triphosphate; dTTP, deoxythymidine 5′-triphosphate.

MuLV RT is more faithful than HIV-1 RT (13–15). Both MuLV and HIV-1 RT proteins lack the 3′ to 5′ proofreading exonuclease activity that many high fidelity host replication DNA polymerases (*i.e.* Polδ) possess. Consequently, the fidelity differences between these two RTs are independent of the 3′ to 5′ exonuclease activity. A similar fidelity difference was also observed between several oncoretroviral (avian myeloblastosis virus RT (13, 16) and bovine leukemia virus RT (17, 18)) and lentiviral RTs (simian immunodeficiency virus RT (12) and equine infectious anemia virus RT (19)), supporting the generalization that oncoretroviral RTs have higher fidelities than lentiviral RTs. These two RTs (MuLV and HIV-1) showed significant differences in mismatch extension fidelity rather than misinsertion fidelity (20). As recently reported, it is becoming increasingly apparent that the fidelity of HIV-1 RT contributes to viral genomic mutagenesis. The primary source of HIV-1 mutagenesis is its RT rather than the host RNA polymerase II that produces the viral genomes (21). Furthermore, we and others have demonstrated that HIV-1 variants harboring high fidelity mutant RTs produce reduced genomic mutation during a single round of viral replication, compared with wild-type virus (21, 22). In addition, human T-cell leukemia virus type I (oncoretrovirus) generates less genomic mutation than HIV-1 during a single round of replication (23).

Thirdly, although the palm and fingers subdomains of these two RTs are structurally very similar, unlike MuLV RT, HIV-1 RT works as a dimer (24, 25). Studies have shown that some equivalent structural residues have different functional roles in HIV-1 and MuLV RTs. When a Phe is substituted for the Tyr^{183} residue in HIV-1 RT, the activity of the resulting mutant enzyme is greatly reduced (26), but the equivalent mutation in MuLV RT (Y222F) does not significantly alter the catalytic activity of the polymerase (27). Finally, these two RTs show different sensitivity to the nucleotide analog, 3TCTP. Whereas wild-type HIV-1 RT is characteristically able to incorporate this chain-terminating substrate, MuLV RT is much less sensitive to this unnatural nucleotide analog (28–30). This difference results from variation in a single amino acid in the conserved Y*X*DD region found in their active sites (YMDD of HIV-1 RT and YVDD of MuLV RT). Consistently, the Val and Ile mutations at the Met^{184} residue of the HIV-1 YMDD sequence are selected during the 3TC treatment (31, 32). In addition, these two 3TC-resistant HIV-1 RT mutants, M184V and M184I, also show increased enzyme fidelity (33–35). These findings suggest that the conserved Y*X*DD region of RTs appears to be important to both 3TCTP selection and enzyme fidelity. Therefore, MuLV and HIV-1 RTs, which are very similar in general, appear to have different local structures and unique enzymatic characteristics.

With the advent of rapid quench techniques, pre-steady-state kinetic assays have been employed to study mechanistic properties of DNA polymerases including RTs. These assays can measure kinetic parameters associated with: 1) polymerase binding to the T/P (K_D), 2) subsequent binding of a dNTP substrate (K_d), and 3) chemical incorporation of the nucleotide onto the primer strand (k_{pol}) (36, 37). Because mutation synthesis is comprised of two mechanistically distinct DNA polymerization events, nucleotide misinsertion (*i.e.* misincorporation) and mismatch extension, we can evaluate the capability of a polymerase to carry out these events by measuring the kinetics for nucleotide incorporation onto both matched and mismatched T/P. These types of studies have shown that HIV-1 RT is relatively efficient at completing both these steps of misincorporation and mismatch extension (38–41). It was also reported that HIV-1 RT distinguishes correct and incorrect dNTPs at both the dNTP binding step (K_d) and the incorporation step (k_{pol}), unlike the Klenow fragment of *Escherichia coli* DNA polymerase I that predominantly uses the k_{pol} step to distinguish between correct and incorrect dNTPs (42).

To further expound upon the foundation laid by the aforementioned studies demonstrating both the similarities and differences between MuLV and HIV-1 RTs, we compared the kinetic mechanisms involved in DNA polymerization and mutation synthesis of MuLV and HIV-1 RTs using pre-steady-state kinetic assays. Here, we compared the kinetic parameters associated with dNTP incorporation, misincorporation and mismatch extension, and T/P binding by MuLV and HIV-1 RTs. Our study reveals that MuLV RT has a much lower binding affinity to both correct and incorrect dNTPs than HIV-1 RT. Overall, the study confirms that the higher fidelity of the MuLV RT is likely due to its reduced ability to complete mismatch extension (20). The implication of these mechanistic discrepancies between MuLV and HIV-1 RTs on viral phenotypic differences is discussed.

EXPERIMENTAL PROCEDURES

Purification of MuLV RT—MuLV RT was overexpressed in *E. coli* BL21 (Novagen) from the pMULVRT plasmid (43). The pMULVRT expression construct encodes for full-length MuLV RT fused at the N terminus to six histidine residues. The hexahistidine-tagged RT was purified using Ni^{2+} chelation chromatography as described previously (43–45). From 1 liter of culture, we were able to purify 4 mg of monomeric MuLV RT. Expression and purification of HIV-1 RT were described previously (44). To examine the purity of the purified RT proteins, 4 μg of the purified RTs were analyzed in 10% SDS-polyacrylamide gels using 4 μg of 98% pure bovine serum albumin (Sigma-Aldrich) as a control. The gels visualized by Coomassie Blue staining were analyzed by a densitometer, and the purified RT proteins showed similar levels of minor contaminants to the bovine serum albumin control, suggesting that the RT proteins used in this study must have at least 95% purity.

Pre-steady-state Kinetic Assays—Pre-steady-state burst and single turnover experiments were performed to examine the transient kinetics associated with incorporating a single nucleotide onto either a matched or mismatched T/P (39). To study the incorporation of each of the four dNTPs (correct), four different ^{32}P-labeled 23-mer primers (matched; A primer, 5′-CGCGCCGAATTCCCGCTAGCAAT-3′; T primer, 5′-CCGAATTCCCGCTAGCAATATTC-3′; G primer, 5′-CGAATTCCCGCTAGCAATATTCT-3′; C primer, 5′-GCCGAATTCCCGCTAGCAATATTCT-3′) were individually annealed to a 38-mer RNA template (5′-GCUUGGCUGCAGAAUAUUGCUAGCGGGAAUUCGGCGCG-3′). Reactions were performed using a Kintek Rapid Quench machine (37, 40, 46). Products were analyzed by 14% denaturing sequencing gel electrophoresis and quantified with the Cyclone phosphorimager (PerkinElmer Life Sciences). Pre-steady-state burst experiments were employed to determine the active site concentrations of the MuLV and HIV-1 RT proteins on the 23-mer T primer annealed to the 38-mer RNA template. In this experiment, 800 μM dTTP was rapidly mixed with RT (50–75 nM active RTs) prebound onto T/P (300 nM). In the pre-steady-state single turnover experiments that measured the dNTP concentration dependence of the purified MuLV RT protein, excess active RT (200 nM) (as determined by the burst experiments) was added to 50 nM T/P.

For studying misinsertion and mismatched primer extension fidelity, either a matched ^{32}P-labeled T primer (matched T primer, 5′-CGCGCCGAATTCCCGC-3′) or a mismatched ^{32}P-labeled G/T primer (5′-CGCGCCGAATTCCCGT-3′) was annealed onto the 38-mer RNA template (see above). This generated a T/P that was identical, except that the 3′ nucleotide on the primer strand of the mismatched T/P was not complementary to the corresponding template nucleotide, which is representative of a mismatched T/P product formed after a misincorporation event. When examining incorrect dNTP incorporation, experiments were carried out manually and at longer time points with higher concentrations of RT (400 nM). The K_d and k_{pol} values of the RTs determined with the 16-mer T primer were similar to those determined with the 23-mer T primer (see Table I and II). The active site concentrations of the RT proteins with the mismatched T/P were also measured using the same protocol as described for the matched 23-mer T-T/P (see above). The same rapid quench protocol was used to perform the mismatched primer extension reactions. The pre-steady-state kinetic data of HIV-1 RT for the misinsertion and mismatched primer extension, which were obtained using the same protocol, have been published in our recent study (39).

Data Analysis—Pre-steady-state kinetic data were analyzed using nonlinear regression. Equations were generated with the program KaleidaGraph version 3.51 (Synergy Software). Data points obtained during the burst experiment were fitted to the burst equation (36, 37).

$$[\text{product}] = \text{Amp}[1 - \exp(-k_{obs}t) + k_{ss}t] \quad \text{(Eq. 1)}$$

The value Amp is the amplitude of the burst, which reflects the actual concentration of enzyme that is in active form. k_{obs} is the observed first-order rate constant for dNTP incorporation whereas k_{ss} is the observed steady-state rate constant (37, 40, 47). Data from single turnover experiments were fit to a single exponential equation that measures the rate of dNTP incorporation (k_{obs}) per given dNTP concentration ([dNTP]). These results were then used to determine K_d, the dissociation constant for dNTP binding to the RT·T/P binary complex, and k_{pol}, the maximum rate of chemical catalysis/conformational change. This was done by fitting the data to the following hyperbolic equation.

$$k_{obs} = k_{pol}[\text{dNTP}]/(K_d + [\text{dNTP}]) \quad \text{(Eq. 2)}$$

From this equation, we could then identify the kinetic constants for each RT during pre-steady-state kinetics: k_{pol}, the maximum rate of dNTP incorporation; and K_d, equilibrium dissociation constant for the interaction of dNTP with the E·DNA complex (37, 41).

Determination of T/P Binding Affinity (K_D)—The protocol for the K_D determination has been described recently (39). Reactions to assess the T/P concentration dependence of the RT proteins were also performed using the Rapid Quench machine. In these experiments, active RT (50 nM) was preincubated with varying concentrations of T/P (10–700 nM). Polymerization was initiated by addition of 800 μM dTTP and allowed to proceed at 37 °C for 250 ms. Product formation was measured and fit into the following quadratic equation.

$$RT - T/P = 0.5(K_D + RT_t + T/P) - 0.5\sqrt{(K_D + RT_t + T/P)^2 - 4RT_tT/P} \quad \text{(Eq. 3)}$$

The variables $RT - T/P$, K_D, RT_t, and T/P reflect productive RT-template concentration, equilibrium dissociation constant for RT binding to T/P, active RT concentration, and total T/P concentration, respectively. From Eq. 3, the K_D values of the MuLV RT to the aforementioned T/Ps were determined (48).

Multiple dNTP Incorporation Assay with Matched and Mismatched Primers—The primer extension assay was modified from a previously described misincorporation assay (49). Briefly, a matched RNA T/P was prepared by annealing the 38-mer RNA template (see above) to the 17-mer A primer (5′-CGCGCCGAATTCCCGCT-3′), and a mismatched RNA T/P was prepared by annealing the 38-mer RNA template with the mismatched G/T primer (see above). In addition, a mismatched DNA T/P was prepared with a 38-mer DNA template encoding the exact nucleotide sequence as the 38-mer RNA template annealed to a mismatched C/A primer (5′-CGCGCCGAATTCCCGCTAA- 3′). All primers used in this assay were ^{32}P-labeled at their 5′ end (template:primer, 2.5:1). Assay mixtures (20 μl) contained 10 nM T/P, the RT protein concentrations showing the primer extension activities described in the individual figure legends, and four dNTPs at the concentrations indicated in the figure legends under the condition described in the pre-steady-state kinetics assay described above. Reactions were incubated at 37 °C for 5 min and terminated for analysis as described in the dNTP assay. Concentrations of RTs (*i.e.* 1–4×) and dNTPs (*i.e.* 4 and 0.04 μM) used in each primer extension experiment were described in each figure legend. Two times more RT activities and 10-min reaction times were used for the mismatched primer extension (2× and 4×, Fig. 5), compared with the matched primer extension reaction (5 min, 1× and 2×, Figs. 3 and 5). These reaction conditions allow multiple rounds of primer extension. Products were resolved using 14% polyacrylamide-urea gel and visualized by phosphorimager.

RESULTS

Active Site Concentrations of MuLV RT on Matched T/P—First, we determined the active concentrations of MuLV RT and HIV-1 RT proteins on ^{32}P-labeled 23-mer T primer annealed to a 38-mer RNA template (T-T/P). We measured product formation when 800 μM correct dTTP is mixed with RT (50–75 nM active RT, see below) prebound onto the T/P (300 nM, excess T/P). There is an initial burst of product formation due to dTTP incorporation onto the prebound RT·T/P complex (pre-steady-state kinetics), which is followed by a slower and linear phase of product formation corresponding to the steady-state kinetics associated with multiple rounds of DNA polymerization. By fitting these results to Eq.1, we see that MuLV RT (Fig. 1*A*) and HIV-1 RT (Fig. 1*B*) are 50% and 32% (74.4 and 48.9 nM) active on the T-T/P, respectively. Additional data obtained from these burst experiments include measures for the rates of DNA polymerization during the pre-steady state (k_{obs}) and steady state (k_{ss}). The MuLV and HIV-1 RT pre-steady-state rates of dTTP incorporation onto the T/P (k_{obs}) were 28.95 and 129.25 s^{-1}, and their rates during the steady state were 0.13 and 0.02 s^{-1}. We also tested a second T-T/P (16-mer T-T/P), which contains different neighboring sequences at the 3′ end of the primers, compared with the 23-mer T-T/P. We observed similar active site concentrations, k_{ss} and k_{obs}, for both RT proteins with the 16-mer T-T/P and the 23-mer T-T/P (data not shown). Basically, like HIV-1 RT and other DNA polymerases, MuLV RT incorporates nucleotides at a faster rate during the pre-steady state than during the steady state.

Pre-steady-state Kinetics of dNTP Incorporation on Matched T/P—Next, we performed single turnover experiments (200 nM active RT and 50 nM T/Ps) to obtain an actual measure for the dNTP incorporation rate at different dNTP concentrations during the pre-steady state. We first assessed the incorporation of four different dNTPs with the four different T/Ps by MuLV and HIV-1 RTs using single turnover experiments. By measuring the dependence of reaction rate (k_{obs}) on five different dNTP concentrations (Fig. 2), we were able to measure the kinetic parameters of K_d, which is the binding affinity of RT to the incoming nucleotide substrate, and k_{pol}, the maximum rate of dNTP incorporation (conformational change and chemical catalysis). As shown in Table I, the binding affinity (K_d) of MuLV RT to dNTPs is 18.1–115.9 μM, and the rate at which it incorporates this nucleotide (k_{pol}) is 47.2–159.3 s^{-1}. Interestingly, whereas the k_{pol} values of MuLV RT are similar to those of HIV-1 RT on these T/Ps, MuLV RT is 6.5–121.6-fold less efficient at binding the incoming dNTP than HIV-1 RT. To confirm this K_d difference, we also employed the 16-mer T-T/P (see above). In this experiment, we also observed a 40.2-fold lower K_d value for MuLV RT (44.2 μM) for dTTP as compared with HIV-1 RT (1.1 μM). Both RT proteins, however, had similar k_{pol} values of 20.0 and 21.7, respectively (Table I). These data confirm the K_d difference between HIV-1 RT and MuLV RT proteins, which was observed with each of the five T/Ps with four dNTPs. Clearly, MuLV RT has a much lower dNTP substrate binding affinity (K_d) than HIV-1 RT, even though both RTs have similar conformational change and catalysis capabilities (k_{pol}), and MuLV RT has 3.5–43.8× less dNTP incorporation efficiency (k_{pol}/K_d, Table I) than HIV-1 RT.

[dNTP]-dependent DNA Synthesis by MuLV and HIV-1 RT Proteins—The pre-steady-state data shown in Fig. 2 and Table I indicate that MuLV RT has very poor dNTP binding affinity, compared with HIV-1 RT. This kinetic difference predicts that the dNTP binding could become a limiting step during steady state and multiple rounds of dNTP incorporation reaction by MuLV RT at low dNTP concentration, but not in the reactions by HIV-1 RT. We tested this prediction using an assay allowing multiple rounds of dNTP incorporations, a situation that better simulates actual DNA synthesis occurring during viral replication. A ^{32}P-labeled 17-mer primer annealed to the 38-mer RNA template was extended at a high [dNTP] (250 μM; see the *first lanes* of each panel in Fig. 3) at 5 min at 37 °C, using concentrations of MuLV and HIV-1 RTs giving ~50% primer extension. The same reaction was repeated with (different decreasing) dNTP concentrations (250 to 0.05 μM). As shown in

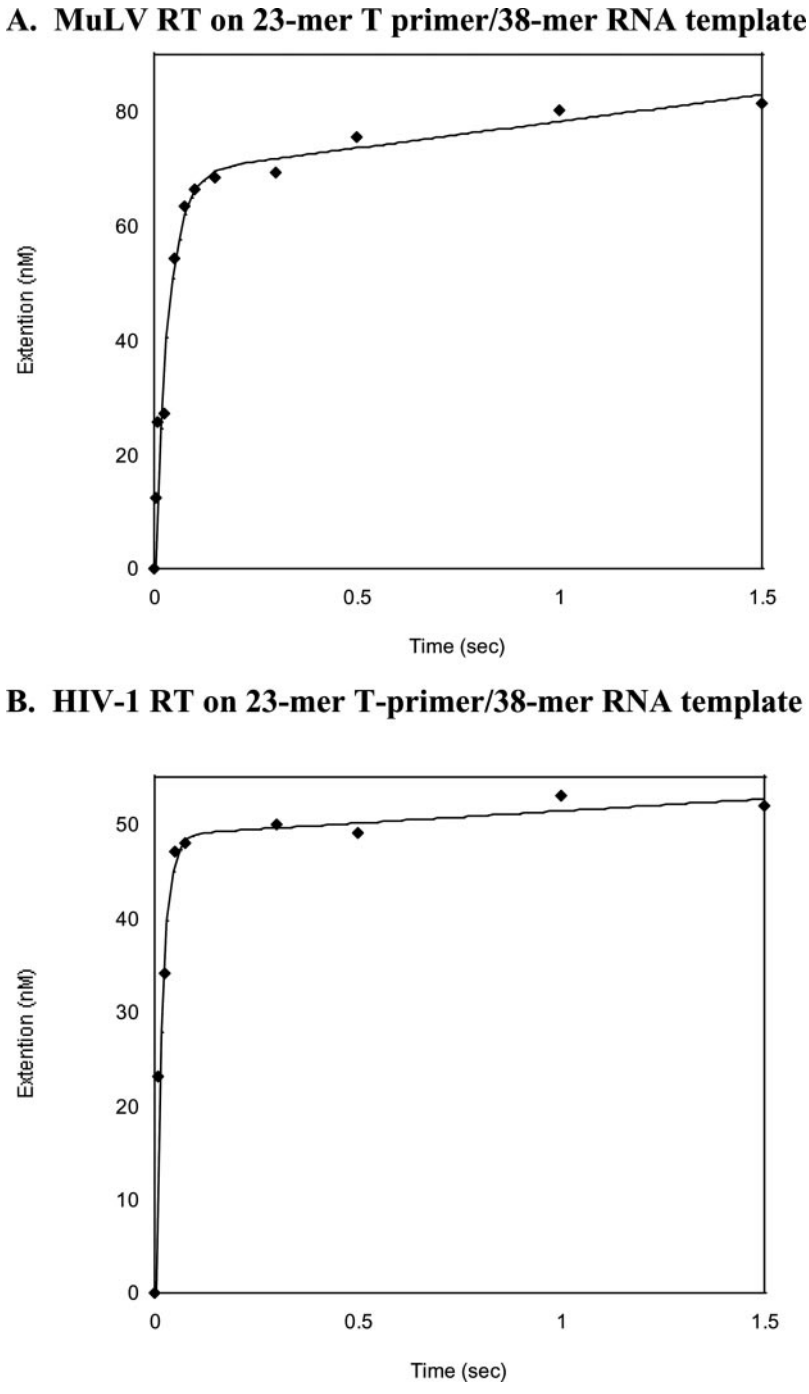

FIG. 1. **Active site titration of MuLV and HIV-1 RT.** Pre-steady-state and steady-state kinetics of MuLV RT (*A*) and HIV-1 RT (*B*) incorporating correct dTTP onto the ^{32}P-labeled 23-mer T primer annealed to the 38-mer RNA template were analyzed. Reactions were carried out at the indicated times by mixing together prebound RT (50–75 nM)·T/P (300 nM) with 800 μM dTTP under rapid quench conditions (see "Experimental Procedures"). The data were fit into the burst equation (Eq. 1) as indicated by the *solid line*, which provides a measure of the active concentration of RT (Amp), the observed first-order rate constant for the burst phase (k_{obs}), and the first-order rate constant for the linear phase (k_{ss}) for MuLV and HIV RT. On the matched T/P, the active concentration (Amp) of MuLV RT was 74.4 ± 0.9 nM. Its k_{obs} was 28.95 ± 5.6 s^{-1}, and its k_{ss} was $1.3 \times 10^{-1} \pm 4.3 \times 10^{-3}$ s^{-1}. On matched T/P, the active concentration (Amp) of HIV-1 RT was 48.9 ± 4.7 nM. Its k_{obs} was 129.25 ± 50.4 s^{-1}, and its k_{ss} was $2.2 \times 10^{-2} \pm 1.6 \times 10^{-2}$ s^{-1}.

Fig. 3, indeed, MuLV RT failed to catalyze DNA synthesis as dNTP concentration was decreased, whereas HIV-1 RT continued to efficiently execute DNA synthesis even at dNTP concentrations as low as 0.1 μM. These data support the prediction that the dNTP binding becomes a rate-limiting step during the multiple-round and multiple nucleotide DNA synthesis by MuLV RT at low dNTP concentrations, presumably due to the low K_d values of MuLV RT.

Pre-steady-state Kinetics of Incorrect dNTP Incorporation—Next, we determined K_d and k_{pol} values with incorrect dNTPs with the matched T primer annealed to the 38-mer RNA template. As expected, a reduction in binding affinity for the nucleotide substrate is seen when examining the incorrect nucleotide incorporation kinetics of these two retroviral RTs, compared with their binding affinity to correct dNTPs. As shown in Fig. 4 and summarized in Table II, MuLV RT incorporates (k_{pol}) incorrect dCTP and dGTP at rates of 0.032 and 0.020 s^{-1}, respectively. These results indicate that MuLV RT chemically incorporates incorrect dNTPs at a rate similar to that seen with HIV-1 RT (Table II). In contrast, MuLV RT is 85.4- and 13.2-fold less efficient at binding incorrect dGTP and dCTP as compared with HIV-1 RT. The binding affinity (K_d) of the MuLV and HIV-1 RTs to incorrect dGTP is 1178.3 and 13.8 μM, respectively. Similarly, the K_d of the MuLV and HIV-1 RTs to incorrect dCTP is 1546.5 and 117.3 μM, respectively. However, the dATP misincorporation was not significant enough to obtain the maximum primer extension, even with the highest dATP concentration that could be used without nonspecific substrate inhibition (2 mM) with this T/P.

Roberts *et al.* (13, 50) previously showed that MuLV RT has a 15-fold higher fidelity than HIV-1 RT. To determine whether

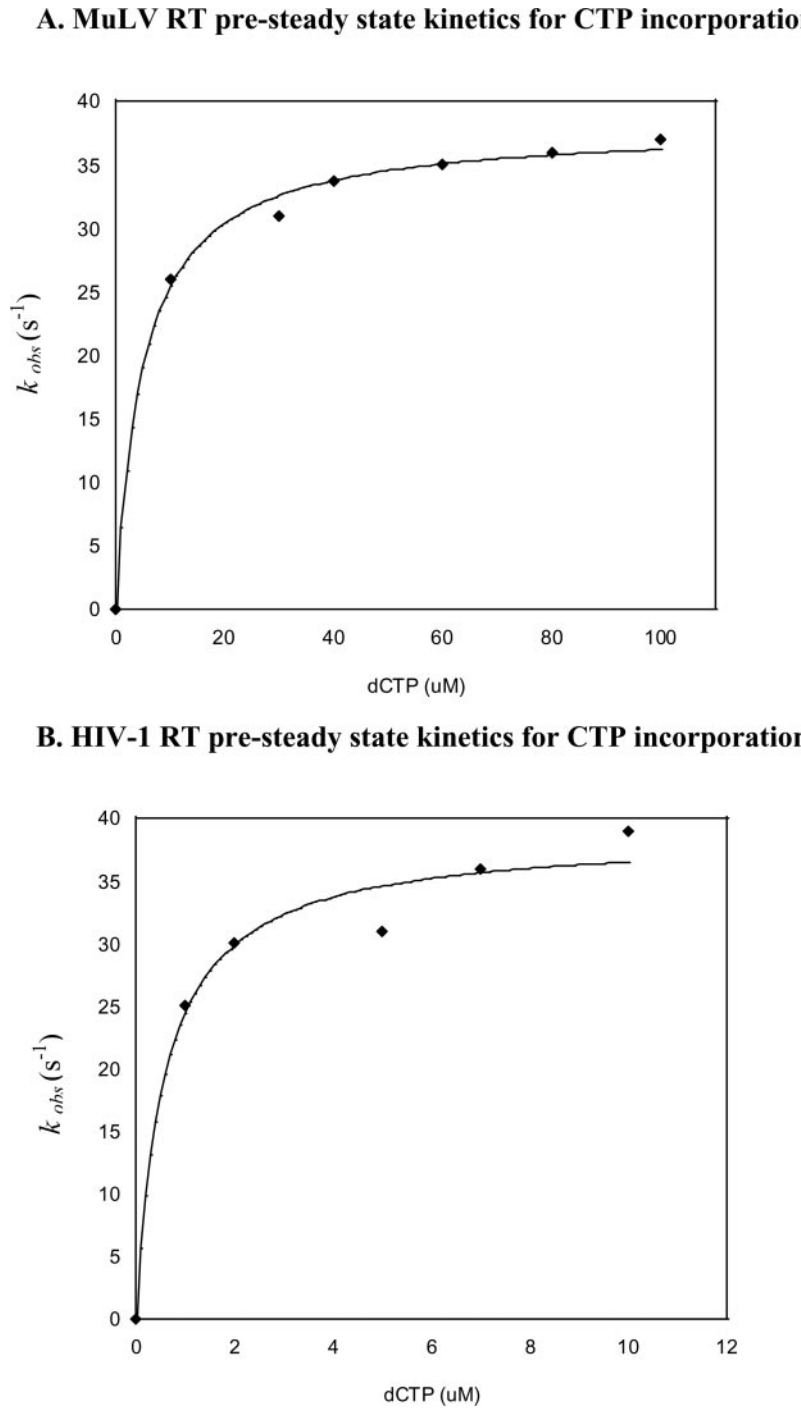

FIG. 2. **Pre-steady-state kinetics of dCTP incorporation by MuLV and HIV-1 RTs on matched T/P.** The ^{32}P-labeled 23-mer C primer annealed to the 38-mer RNA template (50 nM) was extended with excess RT (200 nM) for the single-round dCTP incorporation at five different dCTP concentrations. The k_{obs} value at each dCTP concentration was plotted, and the k_{pol} and K_d values of each RT protein were fit into Eq. 2 as indicated by the *solid line*. The data for dCTP, as well as the other three correct dNTPs, are summarized in Table I. *A*, MuLV RT incorporation of dCTP. *B*, HIV-1 RT incorporation of dCTP.

the high fidelity nature of MuLV RT is due to its ability to discriminate between correct and incorrect nucleotides during the first step of mutation synthesis, we calculated the misinsertion fidelity of this polymerase when incorporating incorrect dGTP and dCTP. In comparison to HIV-1 RT, MuLV RT has either a 3.6-fold higher or 4.0-fold lower misinsertion fidelity for dGTP and dCTP, respectively (Table II). This result suggests that a difference in misinsertion fidelity does not explain the 15-fold higher fidelity of the MuLV RT over HIV-1 RT. In other words, the misinsertion step may not play a significant role in the fidelity difference between these two RTs, which was previously implicated in the steady-state kinetic study (20).

Kinetics Analysis of dNTP Incorporation onto Mismatched T/P with MuLV RT—Since the misinsertion experiment described above suggested that the misinsertion step does not significantly contribute to the fidelity difference between MuLV and HIV RTs, we examined the pre-steady-state kinetics of mismatch extension (or dNTP incorporation from the mismatched primer), the second step of mutation synthesis. We first examined the mismatched primer extension capability of HIV-1 and MuLV RTs using multiple rounds of the mismatched primer extension reaction (Fig. 5). When the same RT activities of HIV-1 and MuLV RTs showing ~40% and 80% (1× and 2×) of the 17-mer matched T/P (see ratios between fully extended primer F and starting matched primer P in Fig. 4*A*; slightly higher RT activities were used for MuLV RT) were used, compared with HIV-1 RT, MuLV RT showed very low capability of extending both G/T and C/A mismatched primers annealed to the 38-mer RNA and DNA templates, respectively.

TABLE I
Pre-steady-state kinetic parameters of HIV-1 and MuLV RTs with four dNTPs

DNTPs	RT	Kinetics parameters (fold differences)[a]		
		k_{pol}	K_d	K_{pol}/K_d
		s^{-1}	μM	$\mu M^{-1}\ s^{-1}$
DCTP	HIV-1	37.5 ± 7.5	0.334 ± 0.4	112.5
	MuLV	47.2 ± 8.1 (×1.3)	18.1 ± 9.4 (×54.2)	2.6 (×43.3)
DATP	HIV-1	33.7 ± 0.6	0.610 ± 0.5	55.3
	MuLV	159.2 ± 4.7 (×4.7)	74.2 ± 1.2 (×121.6)	2.1 (×26.3)
DGTP	HIV-1	39.4 ± 5.6	3.9 ± 0.04	10.2
	MuLV	72.2 ± 3.8 (×1.8)	25.2 ± 8.3 (×6.5)	2.9 (×3.5)
DTTP	HIV-1	36.6 ± 7.5	2.5 ± 1.4	14.6
	MuLV	159.3 ± 14.9 (×4.4)	115.9 ± 9.3 (×46.4)	1.4 (×10.4)
DTTP[b]	HIV-1[c]	21.7 ± 0.7	1.1 ± 0.1	19.7
	MuLV	20.0 ± 0.6 (×1.1)	44.2 ± 4.0 (×40.2)	0.45 (×43.8)

[a] Fold differences of MuLV RT relative to HIV-1 RT.
[b] dTTP incorporation with the 16-mer matched T primer.
[c] Data published previously (39).

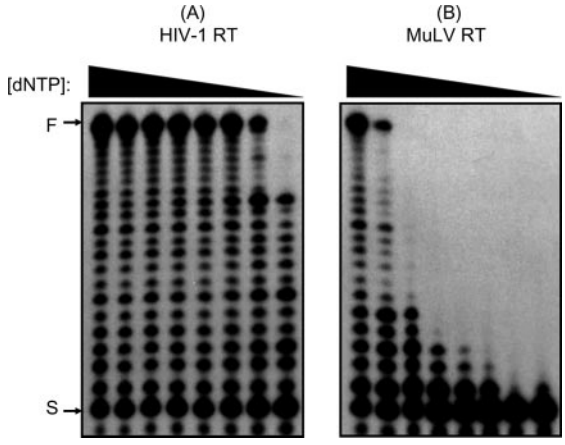

FIG. 3. **Primer extension by HIV-1 and MuLV RTs at different dNTP concentrations.** ^{32}P-labeled 17-mer primer (*S*) annealed to the 38-mer RNA template was incubated with HIV-1 (*A*) and MuLV (*B*) RTs showing 50% of primer extension (*F*) at 37 °C for 5 min with 250 μM dNTP (the highest dNTP concentration). The same reaction was repeated with seven decreasing dNTP concentrations (25, 5, 1, 0.5, 0.25, 0.1, and 0.05 μM). The reactions were analyzed with 14% denaturing polyacrylamide gels.

These data support that the mismatch extension plays an important role in the fidelity difference between these two RTs, as was suggested previously (20).

The protocol for the pre-steady-state kinetic analysis of mismatch extension was described recently in our study for the characterization of several dNTP binding mutants of HIV-1 RT (39). We first determined the active concentration of the RT proteins on the mismatched T/P (G/T mismatched annealed to the 38-mer RNA template). Using the experimental conditions and data analysis protocol described for active site titration on a matched T/P, we see that MuLV RT is 44.9% (67.3 nM) active on mismatched T/P (data not shown). We measured product formation corresponding to dTTP incorporation onto mismatched T/P. Our results with MuLV RT are shown in Fig. 4*C* and summarized in Table III. The data with HIV-1 RT have been reported recently (39) and are shown in the Table III. The first observation to be made is that MuLV RT is less capable of both binding (K_d) and incorporating (k_{pol}) dTTP onto a mismatched T/P in comparison with its ability to carry out polymerization on the matched T-T/P (Tables II and III). In this scenario, during mismatch extension, MuLV RT incorporates dNTP at a maximum rate of $11.6 \times 10^{-3}\ s^{-1}$ and has a binding affinity of 39.4 μM for the dNTP. The mismatch extension of MuLV RT is 137.9-fold less efficient (k_{pol}/K_d) than that of HIV-1 RT. However, because the matched primer extension (incorporation of correct dTTP) of MuLV RT is also 43.8-fold less efficient than that of HIV-1 RT (Table II), the calculated mismatch extension fidelity of MuLV RT (Table III) is 3.1-fold higher than that of HIV-1 RT (Table III).

Interestingly, whereas the mismatched primer extension of MuLV RT is 1552-fold less efficient than its matched primer extension (see k_{pol}/K_d values in incorporation of correct dTTP with matched primer (Table II) and mismatched primers (Table III)), it is 14–17-fold more efficient than the misincorporation efficiency. We also found that, like MuLV RT, the k_{pol}/K_d of HIV-1 RT for correct nucleotide incorporation on matched T/P was greater than the k_{pol}/K_d of mismatch extension, which, in turn, was greater than the k_{pol}/K_d of misincorporation. However, the efficiencies of MuLV RT in catalyzing these three polymerization events are lower than those of HIV-1 RT. In fact, the mismatch extension efficiency of MuLV RT ($2.9 \times 10^{-4}\ \mu M^{-1}\ s^{-1}$; Table III) is as low as the misincorporation efficiency of HIV RT (2.3×10^{-4} to $2.7 \times 10^{-3}\ \mu M^{-1}\ s^{-1}$; Table II). These mechanistic differences between HIV-1 and MuLV RTs are identical with the ones that we observed recently in the pre-steady-state kinetic analyses of wild type and two HIV-1 RT mutants, V148I and Q151N, which specifically lost their binding affinity to the incoming dNTP substrates (39).

Binding Affinity of RT Proteins to T/P—RT binding to T/P is the mechanistic step that precedes nucleotide binding and incorporation. In addition, due to the much lower mismatch extension efficiency of MuLV RT ($2.9 \times 10^{-4}\ \mu M^{-1}\ s^{-1}$), compared with that of HIV-1 RT ($0.04\ \mu M^{-1}\ s^{-1}$), MuLV RT is more likely to fall off from the mismatched primer after the misincorporation step than HIV-1 RT. Consequently, ability to bind mismatched T/P may influence the fidelity of a polymerase. To assess whether MuLV RT differs from HIV-1 RT in its ability to perform this step in polymerization/mutation synthesis, we measured its binding affinity (K_D) to both our matched T primer and our mismatched G/T primer annealed onto an RNA template using the protocol described recently (39). As shown in Table III, the K_D of MuLV RT to mismatched primer was 203.2 nM. Compared with HIV-1 RT, MuLV RT is 3.8-fold less able to bind mismatched T/P (Table III), even though MuLV RT showed a similar K_D to matched primer with HIV-1 RT (data not shown) (39). These results suggest that a diminished capacity to bind mismatched T/P during mismatch extension can additionally contribute to the higher fidelity of the MuLV RT in relation to wild-type HIV-1 RT.

DISCUSSION

We report here the kinetic parameters associated with DNA polymerization and mutation synthesis by MuLV RT on an RNA template. By concomitantly relating these findings to the HIV-1 RT pre-steady-state kinetic results, we provide a com-

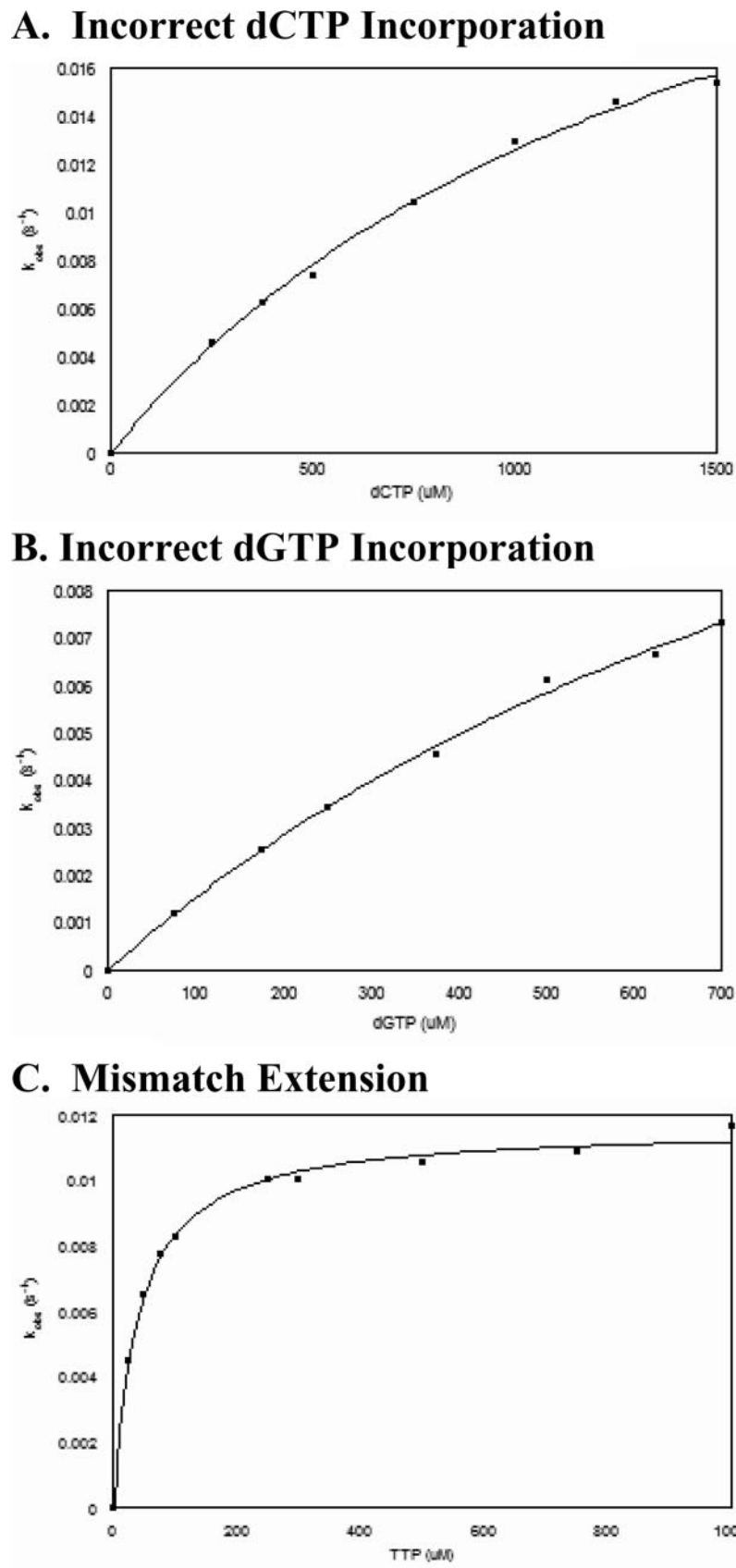

FIG. 4. **MuLV RT pre-steady-state kinetics on misinsertion and mismatch extension.** Assessment of nucleotide incorporation on matched T/P represents events associated with the first step of mutation synthesis, misinsertion. The concentration dependence of MuLV RT for incorrect dCTP (*A*) and incorrect dGTP (*B*) was determined. We measured k_{obs} for each nucleotide at varying concentrations and fit our results into Eq. 2 (indicated by the *solid line*) to calculate the corresponding values of k_{pol} and K_d. The k_{pol} and K_d were 0.032 ± 0.002 s^{-1} and 1546.5 ± 176.7 μM for incorrect dCTP and 0.020 ± 0.002 s^{-1} and 1178.3 ± 169.2 μM for incorrect dGTP. These kinetic data are summarized in Table II. *C*, dTTP incorporation onto a mismatched T/P represents the second step of mutation synthesis, mismatch extension. The concentration dependence of MuLV RT for correct dTTP was determined. We measured k_{obs} for dTTP at varying concentrations and fit our results into Eq. 2 (indicated by the *solid line*) to calculate the corresponding values of k_{pol} and K_d. On mismatched T/P, the k_{pol} and K_d of MuLV RT for correct dTTP was $11.6 \times 10^{-3} \pm 0.1 \times 10^{-3}$ s^{-1} and 39.4 ± 2.3 μM, respectively. These data are summarized in Table III.

prehensive mechanistic comparison of the HIV-1 and MuLV RTs. Firstly, we examined the kinetics for the incorporation of four different dNTPs (correct) by MuLV and HIV-1 RTs. In this experiment, we observed that whereas the k_{pol} values of HIV-1 and MuLV RTs for dNTPs are very similar, MuLV RT binds nucleotide substrates with 6.5–121.6-fold lower affinity than HIV-1 RT. We reasoned that the lower binding affinity of MuLV RT to correct dNTPs may contribute to its higher steady-state K_m values compared with HIV-1 RT (7–11). As shown in our multiple nucleotide incorporation reaction (Fig. 3), MuLV

TABLE II
Pre-steady-state kinetic parameters of HIV-1 and MuLV RTs for misincorporation

dNTP	RT	Kinetic parameters (fold differences)[a]			
		k_{pol}	K_d	k_{pol}/K_d	Misinsertion fidelity[b]
		s^{-1}	μM	$\mu M^{-1}\ s^{-1}$	
DTTP (correct)	HIV-1[c]	21.7 ± 0.7	1.1 ± 0.1	19.7	
	MuLV	20.0 ± 0.6 (×1.1)	44.2 ± 4.0 (×40.2)	0.45 (×43.8)	
DGTP (incorrect)	HIV-1[c]	0.037 ± 0.001	13.8 ± 2.2	2.7×10^{-3}	7296.3
	MuLV	0.020 ± 0.002 (×1.9)	1178.3 ± 169.2 (×85.4)	1.7×10^{-5} (×158.8)	26470.6 (×3.6)
DCTP (incorrect)	HIV-1[c]	0.027 ± 0.001	117.3 ± 7.3	2.3×10^{-4}	85652.2
	MuLV	0.032 ± 0.002 (×1.2)	1546.5 ± 176.7 (×13.2)	2.1×10^{-5} (×10.9)	21428.6 (×0.25)

[a] Fold differences of MuLV RT relative to HIV-1 RT.
[b] $(k_{pol}/K_d)_{correct}/(k_{pol}/K_d)_{incorrect}$.
[c] Data published previously (39).

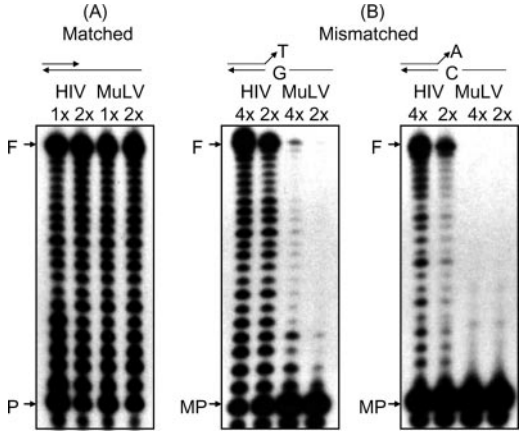

FIG. 5. **Mismatch extension capability of MuLV and HIV-1 RTs.** *A*, the ^{32}P-labeled matched primer (*P*) annealed to the 38-mer RNA template was extended by two different concentrations of HIV-1 and MuLV RTs showing ~35% (1×) and 70% (2×) of the primer extension (*F*) at 37 °C for 5 min with 250 μM dNTP. *B*, the primer extension reactions were repeated with either G/T (*left panel*) or C/A (*right panel*) mismatched primer (*MP*) annealed to the 38-mer RNA or DNA template, respectively, under the same conditions used in the matched T/P reactions (*A*), except for twice more RT activity (2× and 4×). The reactions were analyzed with 15% denaturing polyacrylamide gels.

RT clearly displayed a great reduction of the DNA synthesis at low dNTP concentrations. It is possible that, when the dNTP availability is low, the dNTP binding step of MuLV RT becomes rate-limiting, which reduces its capability of executing multiple nucleotide incorporations that normally occur during viral DNA synthesis. We recently demonstrated that MuLV RT also shows lower dNTP incorporation efficiency than HIV-1 RT under a single round of processive DNA synthesis at low dNTP concentrations (*i.e.* 40 nM) (6). In contrast, due to the tight dNTP binding affinity of HIV-1 RT, this RT protein is still able to retain synthesis activity, even at low dNTP concentrations. This is also consistent with the low steady-state K_m values of HIV-1 RT, compared with those of MuLV RT (6–8). The same multiple nucleotide incorporation difference seen between HIV-1 and MuLV RTs (Fig. 3) was also observed between the wild type and two dNTP binding mutants (Q151N and V148I) of HIV-1 RT (6). Models suggested that these two mutations disrupt the interaction between the RT active site and the 3′ OH of the incoming dNTP substrate, resulting in an increase of the K_d values without affecting the k_{pol} values (39). Basically, these two dNTP binding HIV-1 RT mutant proteins kinetically mimic MuLV RT in DNA polymerization.

Here, using a series of virological and cellular aspects related with these two different retroviruses, MuLV and HIV-1, we envision possible significances of the dNTP binding difference between these two RTs. Firstly, HIV-1, which is a lentivirus, uniquely infects not only dividing cells (*i.e.* activated CD4+ T cells) but also nondividing/terminally differentiated cells (mature macrophages), whereas MuLV, an oncoretrovirus, requires proliferating cells (4). Macrophage infection, which is observed in the early asymptomatic phase of HIV-1 infection, is a hallmark phenotype of HIV-1 pathogenesis. Secondly, numerous studies have reported that nondividing cells have much lower cellular dNTP concentrations than dividing cells (5). Using a novel dNTP assay, we recently demonstrated that the dNTP concentration of human mature macrophages is ~40 nM, which is ~100-fold lower than that of activated CD4+ T cells (2–5 μM) (6). More importantly, the steady-state K_m values of HIV-1 and MuLV RTs lie near the cellular dNTP concentrations found in macrophages and activated T cells, respectively. Considering all these findings, we can speculate that the tight binding of the HIV-1 active site to the incoming dNTP substrate may contribute to the unique capability of HIV-1 to infect nondividing cells containing low cellular dNTP concentrations. Conversely, the active site of MuLV RT may have adapted to the high dNTP concentration environments found in the dividing cells that MuLV normally infects. This possibility is further supported by our recent observation that HIV-1 variants harboring RT mutants (V148I and Q151N), which kinetically mimic MuLV RT due to their reduced dNTP binding affinity, failed to infect macrophages even though these mutant viruses normally infect dividing cells (*i.e.* activated CD4+ T cells and transformed cell lines) (6).

Pre-steady-state kinetic study on the M184V 3TC-resistant HIV-1 RT mutant demonstrated that the M184V mutation, which lies near the active site containing the conserved YXDD sequence, slightly increases K_d values (2–6-fold) to dCTP (41), which may explain low infectivity in cells with low dNTP contents (51, 52). This mutant RT also has reduced processivity (53), compared with wild-type HIV-1 RT, which could be responsible for lower infectivity of this mutant virus in primary cells (53, 54). Pre-steady-state kinetic analysis on M184I, which only transiently appears during the 3TC treatment, has not been reported. Interestingly, unlike M184V, M184I has noticeable decreases in the DNA synthesis at low dNTP concentrations,[2] supporting that M184I RT, which has a longer β-branched side chain than the Val mutation, may also affect the binding of dNTP to the active site as observed in Q151N and V148I. Our recent pre-steady-state kinetic analysis showed that RT of simian immunodeficiency virus, another lentivirus infecting nondividing cells, also has lower K_d values, like HIV-1 RT (49). Additionally, we observed that RT of feline leukemia virus (an oncoretrovirus) has higher K_m values than RT of feline immunodeficiency virus (a lentivirus).[2] These combined findings support the idea that the dNTP utilization effi-

[2] M. Skasko, K. K. Weiss, H. M. Reynolds, V. Jamburuthugoda, K. Lee, and B. Kim, unpublished observations.

TABLE III
Pre-steady state kinetic parameters of dTTP incorporation by HIV-1 and MuLV RTs and binding affinity of MuLV and HIV-1 RTs for mismatched T/P

RT	k_{pol}	K_d	k_{pol}/K_d	Mismatch extension fidelity[a]	Binding affinity (K_d) to mismatched T/P[b]
	s^{-1}	μM	$\mu M^{-1}\ s^{-1}$		$n M$
HIV-1[c]	$0.5 \pm 5.6 \times 10^{-3}$	14.1 ± 0.6	0.04	493.5	53.8 ± 2.8
MuLV	$11.6 \times 10^{-3} \pm 0.1 \times 10^{-3}$ (×43.1)[d]	39.4 ± 2.3 (×2.8)[d]	2.9×10^{-4} (×137.9)[d]	1552.7 (×3.1)[d]	203.2 ± 7.6 (×3.8)

[a] $(k_{pol}/K_d)_{matched}/(k_{pol}/K_d)_{mismatched}$.
[b] K_d values were obtained using Eq. 3 as described previously (48).
[c] Data published previously (39).
[d] Fold difference in fidelity relative to wild-type HIV-1 RT.

ciency and dNTP binding affinity of RTs contribute to the host cell specificity of retroviruses. The generality of this idea needs to be further explored by analyzing more RT proteins isolated from different retroviruses. Furthermore, note that, in order to complete viral replication in nondividing cells, HIV-1 also requires a viral accessory protein, viral protein R (Vpr), which enables the pre-integration complex containing the synthesized proviral DNA to enter the nucleus through the nuclear membrane that remains intact in nondividing cells (55, 56). In contrast, other retroviruses, which infect dividing cells, do not require this transport mechanism because the pre-integration complex of these viruses can access chromosomes during mitosis where the nuclear membrane barrier disintegrates.

Both MuLV and HIV-1 RTs displayed similar characteristics in dNTP binding and catalysis during misinsertion events. Whereas the rate (k_{pol}) at which MuLV RT incorporates incorrect dNTPs is comparable with that observed with HIV-1 RT, the binding affinity (K_d) of MuLV RT for incorrect dNTPs is 13.2–85.4-fold lower than that of HIV-1 RT. However, because MuLV RT has diminished binding affinity (K_d) for both correct and incorrect dNTPs, there is a simultaneous reduction in its efficiency (k_{pol}/K_d) of correct and incorrect dNTP incorporation. The net effect is that HIV-1 and MuLV RTs have similar misinsertion fidelities (Table II).

The differences between these two RTs became apparent when we measured the kinetics of mismatch extension for MuLV RT. When incorporating correct dNTP onto a mismatched T/P, this polymerase is altered in its ability to bind (K_d) and catalyze the incorporation (k_{pol}) of the nucleotide substrate, even though the primary difference between these RTs is the rate (k_{pol}) at which they carry out mismatch extension. HIV-1 RT incorporates dTTP onto a mismatched T/P at a maximum rate of 0.45 s^{-1}, which is 43.8-fold faster than the rate of mismatch extension observed with the MuLV RT. The changes in dNTP binding and chemical catalysis translate into a 137.9-fold reduction in mismatch extension efficiency (k_{pol}/K_d) for MuLV RT in comparison with HIV-1 RT. The fact that MuLV RT is so inefficient at carrying out mismatch extension supports the likelihood that the polymerase stalls and falls off the mismatched T/P substrate. In this scenario, it is necessary to assess the capability of MuLV RT to rebind the mismatched T/P. We show that MuLV RT has a 3.8-fold lower binding affinity for mismatched T/P (K_D) than HIV-1 RT. This result indicates that the overall higher fidelity of MuLV RT relative to HIV-1 RT is due to multiple effects of 1) a 3.1-fold higher mismatch extension fidelity and 2) a 3.8-fold reduced ability to rebind mismatched T/P when RT disassociates from the T/P substrate. Due to a 137.9-fold less efficient mismatch extension and poor binding to mismatched T/P, MuLV RT may more likely release from the mismatched T/P after misinsertion. This could create an additional mechanistic barrier that could slow down the mismatch extension step as observed in Fig. 5 and overall mutation synthesis by MuLV RT. In contrast, due to the tighter binding affinity to the mismatched primer and highly efficient capability to extend the mismatched primer, relative to MuLV RT, HIV-1 RT may be able to continue the mismatch extension without falling off from the mismatched T/P, which can lead to high success in the completion of the mutation synthesis by HIV-1 RT.

Using fingerprinting and sequencing analysis of proviral DNA, Monk *et al.* (57) reported that MuLV infection of a clonal cell line yielded a mutation rate of 2×10^{-5} bases per replication cycle. Using the cell-free M13 *lac*Zα forward mutation assay, Roberts *et al.* (50) reported that the MuLV RT had an error rate of 1/30,000, which can account for the estimated *in vivo* MuLV mutation rate published in the aforementioned study. Nevertheless, Roberts *et al.* (50) did report that the error rate of MuLV RT is ~15-fold higher than that of HIV-1 RT, and our findings suggest that the mechanism responsible for this fidelity difference is their differing abilities to complete the process of mismatch extension. The idea that mismatch extension plays an important role in determining the overall fidelity of retroviral RTs was established in 1989 when Perrino *et al.* (58) reported that HIV-1 RT is 50-fold more efficient than DNA polymerase α at synthesizing DNA from a mismatched T/P. This property was characterized in a more quantitative manner when Bakhanashvili and Hizi (20, 59) measured the steady-state kinetics of mismatch extension for both HIV-1 and MuLV RTs. When they measured the mismatch extension capabilities of these two polymerases with three different mismatched T/Ps, the authors reported that the relative mismatch extension frequencies of MuLV RT were, on average, 2–3-fold lower than those seen with HIV-1 RT.

The fact that HIV-1 RT is very efficient (k_{pol}/K_d) at carrying out mismatch extension emphasizes the underlying differences between HIV-1 RT and other retroviral polymerases. The viral polymerase of HIV-1 must have evolved so that its active site is more permissive to introducing mutations into the viral genome. Interestingly, our laboratory has recently identified a molecular interaction within the HIV-1 RT active site that influences how efficiently this polymerase is able to complete the second step of mutation synthesis (39, 45). The Gln^{151} residue is part of the highly conserved LPQG motif found in all retroviral RTs. Previous studies have shown that the interaction between this residue and the dNTP substrate is a determinant for HIV-1 RT fidelity (26, 45, 46, 60, 61). When we performed a comprehensive analysis on the Q151N mutant RT in order to assess its mutation synthesis capabilities, we discovered that alterations in the Gln^{151} residue reduced the efficiency with which HIV-1 RT incorporated correct dNTP into both matched and mismatched T/Ps (39). More specifically, Q151N has a higher K_d value and a lower k_{pol} value than wild-type HIV-1 RT during mismatch extension, as observed in this study with MuLV RT. In addition, whereas Q151N has a reduced K_d (but not k_{pol}) value for both correct and incorrect dNTPs compared with wild-type HIV-1 RT, Q151N does not alter the binding affinity to matched or mismatched primers. This finding suggested that the interactions between Gln^{151}

and the dNTP substrate within the HIV-1 RT active site appear to influence how efficiently this polymerase is able to complete mismatch extension. Interestingly, however, these mechanistic differences between wild-type and Q151N HIV-1 RT proteins are very similar to those observed between HIV-1 and MuLV RTs. This indicates that the active site of the Q151N dNTP binding mutant HIV-1 RT kinetically functions more like the active site of MuLV RT. A similar interaction may occur within the MuLV RT active site, given that it encodes an equivalent residue, Gln^{190}. Biochemical data showing that alterations (Q190N) in this residue can increase the fidelity of the MuLV RT suggest that this residue has the same functional role in both the HIV-1 and MuLV RTs (28, 30). However, given the dramatic difference in the mismatch extension fidelities between the wild-type proteins of these two RTs, it is plausible that there exist interactions (in addition to those with Gln^{151}) between HIV-1 RT and the mismatch extension intermediates that are not present in the MuLV RT.

In addition to Q151N and V148I, the fidelity of the M184V HIV-1 RT, which renders 3TC resistance, has been characterized by pre-steady-state kinetic analysis (41). The M184V HIV-1 RT, which showed an ~2-fold increase fidelity in M13 *lac*Zα forward mutation assay (62), showed a maximum 2.4× higher fidelity than wild-type RT in the kinetic analysis. Interestingly, the K_d increase contributes to the high fidelity nature of M184V. In addition, M184V HIV-1 RT also showed reduced mismatch primer extension capability (63). M184I HIV-1 RT showed slightly higher fidelity than M184V (62). However, the pre-steady-state kinetic analysis has not been reported. A number of other HIV-1 RT mutations altering enzyme fidelity were isolated: D76V (64), R78A (65), E89G (63), and the residues in the minor groove binding track (66, 67). Structural models on D76V, R78A, and E89G suggested that these mutations may affect the RT interaction with template, whereas the minor groove binding track residues interact with the minor groove of the T/P, where the transition from A to B DNA and bending occur. Our pre-steady-state kinetic study shows that D76V and R78A do not show any altered K_d and k_{pol} values,[2] which is consistent with the previous report that these mutations mainly affect RT binding to the single-stranded part of the primer (64, 65). Mutations in the minor groove binding track region (*i.e.* Gly^{266} and Trp^{266}) mainly affect replication frameshift mutation and processivity through altering the RT interaction with the minor groove of the double-stranded T/P. Basically, these studies with the RT mutants with altered fidelity suggest that the RT interaction with substrates, dNTP and T/P, is a key determinant for RT fidelity.

In summary, this is the first time that a comprehensive pre-steady-state kinetic analysis of dNTP incorporation and mutation synthesis by MuLV RT has been reported. The mechanistic analysis of HIV-1 and MuLV RTs clearly sheds lights on the functional and evolutionary relatedness between the dNTP interactions within the RT active site and the virological characteristics of retroviruses such as cell type specificity and genomic mutagenesis.

Acknowledgments—We are thankful to Drs. Robert A. Bambara, Vandana Purohit, and Mini Balakrishnan for thoughtful discussion.

REFERENCES

1. Fields, B. N., Knipe, D. M., and Howley, P. M. (1996) *Fields Virology*, 3rd ed., Lippincott-Raven Publishers, New York
2. De Clercq, E. (1992) *AIDS Res. Hum. Retroviruses* **8,** 119–134
3. Lewis, P., Hensel, M., and Emerman, M. (1992) *EMBO J.* **11,** 3053–3058
4. Lewis, P. F., and Emerman, M. (1994) *J. Virol.* **68,** 510–516
5. Traut, T. W. (1994) *Mol. Cell. Biochem.* **140,** 1–22
6. Diamond, T. L., Roshal, M., Jamburuthugoda, V. K., Reynolds, H. M., Merriam, A. R., Lee, K. Y., Balakrishnan, M., Bambara, R. A., Planelles, V., Dewhurst, S., and Kim, B. (2004) *J. Biol. Chem.* **279,** 51545–51553.
7. Chowdhury, K., Kaushik, N., Pandey, V. N., and Modak, M. J. (1996) *Biochemistry* **35,** 16610–16620
8. Furge, L. L., and Guengerich, F. P. (1997) *Biochemistry* **36,** 6475–6487
9. Shi, Q., Singh, K., Srivastava, A., Kaushik, N., and Modak, M. J. (2002) *Biochemistry* **41,** 14831–14842
10. Ueno, T., Shirasaka, T., and Mitsuya, H. (1995) *J. Biol. Chem.* **270,** 23605–23611
11. Woodside, A. M., and Guengerich, F. P. (2002) *Biochemistry* **41,** 1027–1038
12. Diamond, T. L., Kimata, J., and Kim, B. (2001) *J. Biol. Chem.* **276,** 23624–23631
13. Roberts, J. D., Preston, B. D., Johnston, L. A., Soni, A., Loeb, L. A., and Kunkel, T. A. (1989) *Mol. Cell. Biol.* **9,** 469–476
14. Bebenek, K., Abbotts, J., Roberts, J. D., Wilson, S. H., and Kunkel, T. A. (1989) *J. Biol. Chem.* **264,** 16948–16956
15. Preston, B. D., Poiesz, B. J., and Loeb, L. A. (1988) *Science* **242,** 1168–1171
16. Battula, N., and Loeb, L. A. (1974) *J. Biol. Chem.* **249,** 4086–4093
17. Perach, M., and Hizi, A. (1999) *Virology* **259,** 176–189
18. Avidan, O., Meer, M. E., Oz, I., and Hizi, A. (2002) *Eur. J. Biochem.* **269,** 859–867
19. Bakhanashvili, M., and Hizi, A. (1993) *Biochemistry* **32,** 7559–7567
20. Bakhanashvili, M., and Hizi, A. (1992) *Biochemistry* **31,** 9393–9398
21. O'Neil, P. K., Sun, G., Yu, H., Ron, Y., Dougherty, J. P., and Preston, B. D. (2002) *J. Biol. Chem.* **277,** 38053–38061
22. Mansky, L. M., Le Rouzic, E., Benichou, S., and Gajary, L. C. (2003) *J. Virol.* **77,** 2071–2080
23. Mansky, L. M. (2000) *J. Virol.* **74,** 9525–9531
24. Hsiou, Y., Ding, J., Das, K., Clark, A. D., Jr., Hughes, S. H., and Arnold, E. (1996) *Structure* (*Lond.*) **4,** 853–860
25. Georgiadis, M. M., Jessen, S. M., Ogata, C. M., Telesnitsky, A., Goff, S. P., and Hendrickson, W. A. (1995) *Structure* (*Lond.*) **3,** 879–892
26. Harris, D., Kaushik, N., Pandey, P. K., Yadav, P. N., and Pandey, V. N. (1998) *J. Biol. Chem.* **273,** 33624–33634
27. Kaushik, N., Singh, K., Alluru, I., and Modak, M. J. (1999) *Biochemistry* **38,** 2617–2627
28. Singh, K., Kaushik, N., Jin, J., Madhusudanan, M., and Modak, M. J. (2000) *Protein Eng.* **13,** 635–643
29. Kaushik, N., Talele, T. T., Pandey, P. K., Harris, D., Yadav, P. N., and Pandey, V. N. (2000) *Biochemistry* **39,** 2912–2920
30. Jin, X., Bauer, D. E., Tuttleton, S. E., Lewin, S., Gettie, A., Blanchard, J., Irwin, C. E., Safrit, J. T., Mittler, J., Weinberger, L., Kostrikis, L. G., Zhang, L., Perelson, A. S., and Ho, D. D. (1999) *J. Exp. Med.* **189,** 991–998
31. Wainberg, M. A., Hsu, M., Gu, Z., Borkow, G., and Parniak, M. A. (1996) *AIDS* **10,** S3–S10
32. Faraj, A., Agrofoglio, L. A., Wakefield, J. K., McPherson, S., Morrow, C. D., Gosselin, G., Mathe, C., Imbach, J. L., Schinazi, R. F., and Sommadossi, J. P. (1994) *Antimicrob. Agents Chemother.* **38,** 2300–2305
33. Wainberg, M. A., Drosopoulos, W. C., Salomon, H., Hsu, M., Borkow, G., Parniak, M., Gu, Z., Song, Q., Manne, J., Islam, S., Castriota, G., and Prasad, V. R. (1996) *Science* **271,** 1282–1285
34. Drosopoulos, W. C., and Prasad, V. R. (1998) *J. Virol.* **72,** 4224–4230
35. Rezende, L. F., Curr, K., Ueno, T., Mitsuya, H., and Prasad, V. R. (1998) *J. Virol.* **72,** 2890–2895
36. Johnson, K. A. (1993) *Annu. Rev. Biochem.* **62,** 685–713
37. Johnson, K. A. (1995) *Methods Enzymol.* **249,** 38–61
38. Zinnen, S., Hsieh, J. C., and Modrich, P. (1994) *J. Biol. Chem.* **269,** 24195–24202
39. Weiss, K. K., Chen, R., Skasko, M., Reynolds, H. M., Lee, K., Bambara, R. A., Mansky, L. M., and Kim, B. (2004) *Biochemistry* **43,** 4490–4500
40. Kati, W. M., Johnson, K. A., Jerva, L. F., and Anderson, K. S. (1992) *J. Biol. Chem.* **267,** 25988–25997
41. Feng, J. Y., and Anderson, K. S. (1999) *Biochemistry* **38,** 9440–9448
42. Carroll, S. S., Cowart, M., and Benkovic, S. J. (1991) *Biochemistry* **30,** 804–813
43. Malboeuf, C. M., Isaacs, S. J., Tran, N. H., and Kim, B. (2001) *BioTechniques* **30,** 1074–1078, 1080, 1082, passim
44. Kim, B. (1997) *Methods* (*Orlando*) **12,** 318–324
45. Weiss, K. K., Isaacs, S. J., Tran, N. H., Adman, E. T., and Kim, B. (2000) *Biochemistry* **39,** 10684–10694
46. Weiss, K. K., Bambara, R. A., and Kim, B. (2002) *J. Biol. Chem.* **277,** 22662–22669
47. Kerr, S. G., and Anderson, K. S. (1997) *Biochemistry* **36,** 14064–14070
48. Suo, Z., and Johnson, K. A. (1997) *Biochemistry* **36,** 12459–12467
49. Diamond, T. L., Souroullas, G., Weiss, K. K., Lee, K. Y., Bambara, R. A., Dewhurst, S., and Kim, B. (2003) *J. Biol. Chem.* **278,** 29913–29924
50. Roberts, J. D., Bebenek, K., and Kunkel, T. A. (1988) *Science* **242,** 1171–1173
51. Back, N. K., Nijhuis, M., Keulen, W., Boucher, C. A., Oude Essink, B. O., van Kuilenburg, A. B., van Gennip, A. H., and Berkhout, B. (1996) *EMBO J.* **15,** 4040–4049
52. Miller, M. D., Anton, K. E., Mulato, A. S., Lamy, P. D., and Cherrington, J. M. (1999) *J. Infect. Dis.* **179,** 92–100
53. Harris, D., Yadav, P. N., and Pandey, V. N. (1998) *Biochemistry* **37,** 9630–9640
54. Naeger, L. K., Margot, N. A., and Miller, M. D. (2001) *Antivir. Ther.* **6,** 115–126
55. de Noronha, C. M., Sherman, M. P., Lin, H. W., Cavrois, M. V., Moir, R. D., Goldman, R. D., and Greene, W. C. (2001) *Science* **294,** 1105–1108
56. Sherman, M. P., de Noronha, C. M., Eckstein, L. A., Hataye, J., Mundt, P., Williams, S. A., Neidleman, J. A., Goldsmith, M. A., and Greene, W. C. (2003) *J. Virol.* **77,** 7582–7589
57. Monk, R. J., Malik, F. G., Stokesberry, D., and Evans, L. H. (1992) *J. Virol.* **66,** 3683–3689
58. Perrino, F. W., Preston, B. D., Sandell, L. L., and Loeb, L. A. (1989) *Proc. Natl. Acad. Sci. U. S. A.* **86,** 8343–8347
59. Bakhanashvili, M., and Hizi, A. (1993) *FEBS Lett.* **319,** 201–205

60. Kaushik, N., Harris, D., Rege, N., Modak, M. J., Yadav, P. N., and Pandey, V. N. (1997) *Biochemistry* **36,** 14430–14438
61. Sarafianos, S. G., Pandey, V. N., Kaushik, N., and Modak, M. J. (1995) *Biochemistry* **34,** 7207–7216
62. Rezende, L. F., Drosopoulos, W. C., and Prasad, V. R. (1998) *Nucleic Acids Res.* **26,** 3066–3072
63. Hamburgh, M. E., Drosopoulos, W. C., and Prasad, V. R. (1998) *Nucleic Acids Res.* **26,** 4389–4394
64. Kim, B., Hathaway, T. R., and Loeb, L. A. (1998) *Biochemistry* **37,** 5831–5839
65. Kim, B., Ayran, J. C., Sagar, S. G., Adman, E. T., Fuller, S. M., Tran, N. H., and Horrigan, J. (1999) *J. Biol. Chem.* **274,** 27666–27673
66. Beard, W. A., Bebenek, K., Darden, T. A., Li, L., Prasad, R., Kunkel, T. A., and Wilson, S. H. (1998) *J. Biol. Chem.* **273,** 30435–30442
67. Latham, G. J., Forgacs, E., Beard, W. A., Prasad, R., Bebenek, K., Kunkel, T. A., Wilson, S. H., and Lloyd, R. S. (2000) *J. Biol. Chem.* **275,** 15025–15033